# Subsidence history of the Gunsan Basin (Cretaceous-Cenozoic) in the Yellow Sea, offshore Korea

Eun Young LEE

Department Petroleum Resources Technology, University of Science & Technology, Gwahangno 113,

Yuseong-gu, Daejeon, South Korea;

Current address: Department of Geodynamics & Sedimentology, University of Vienna, Althanstrasse 14, 1090 Vienna, Austria;

queenily2@gmail.com

## Abstract

Rifting in the Gunsan Basin between China and Korea started in late Mesozoic times, due to large-scale interaction between the Pacific, Eurasian and Indian plates. To analyze the detailed tectonic evolution of this basin, backstripping the subsidence history of four representative units in the basin has been undertaken including sag and half-graben structures in the Central sub-basin as well as half-graben and graben structures in the SW sub-basin. Backstripping indicates that the subsidence history of the Gunsan Basin can be grouped into a Late Cretaceous-Oligocene a main subsidence phase and a Middle Miocene-present secondary subsidence phase. These phases were separated by an uplift and erosion phase during early Miocene times. The main subsidence phase comprised a rapid Late Cretaceous-Paleocene subsidence event and a slower Eocene-Oligocene subsidence event. These phases can be correlated to seismic sequence MSQ I, II and III, identified in the SW sub-basin from seismic stratigraphy, and can further be related to the convergence of the Pacific, Eurasian and Indian plates. Compared with the McKenzie (1978) lithospheric stretching model, this basin is relatively similar to the typical tectonic subsidence characteristics of intracontinental basins.

Die Riftingphase im Gunsan Becken zwischen China und Korea begann im späten Mesozoikum als Produkt der Wechselwirkung zwischen Pazifischer, Eurasischer und Indischer Platte. Um die detaillierte tektonische Geschichte des Beckens zu analysieren wurde eine Backstripping-Subsidenzanalyse an vier repräsentativen Einheiten des Beckens unternommen welche, etwa. Mulden- und Halbgrabenstrukturen im zentralen Teilbecken und Halbgräben und Gräben im südwestlichen Teilbecken beinhalten. Die Backstripping-Methode zeigt, dass die Subsidenzgeschichte des Gunsan Beckens in eine Oberkreide-Oligozäne Hauptabsenkungsphase und eine Mittelmiozäne-rezente sekundäre Absenkungsphase geteilt werden kann. Diese Phasen sind durch eine frühmiozäne Phase von Uplift und Erosion getrennt. Die Hauptabsenkungsphase teilt sich in eine Oberkreide-Paleozäne Phase rascher Subsidenz und einen langsameren, Eozän-Oligozänen Abschnitt. Die unterschiedlichen Phasen können mit den seismischen Sequenzen MSQ I, II und III korreliert werden, die im südwestlichen Teilbecken mit Hilfe von seismischer Stratigraphie identifiziert wurden, und können mit der Konvergenz der Pazifischen, Eurasischen und Indischen Platte in Zusammenhang gebracht werden. Im Vergleich mit dem McKenzie (1978) Modell lithosphärischer Dehnung kann das Becken mit der tektonischen Subsidenz intrakontinentaler Becken verglichen werden.

## 1. Introduction

The Yellow Sea, a semi-enclosed continental shelf basin situated between China and Korea (Fig. 1) consists of several basins, including the Bohai, the North Yellow Sea, the South Yellow Sea and the Subei basins. The South Yellow Sea Basin is further subdivided into the Northern and Southern South Yellow Sea basins by a central uplifted area (Zhang et al., 1989). The Gunsan Basin is the Korean portion of the Northern South Yellow Sea Basin (Park et al., 1997) (Fig. 1 and 2).

During the last few decades, comprehensive research programs on the Gunsan Basin have focused primarily on oil exploration. However, the kinematic processes and geodynamic evolution of this basin are far from being understood, although the basin type and rifting processes have been discussed. Marathon (1987) developed a transtensional model for the rifting mechanism. In contrast, Baag and Baag (1994) suggested a suite of pull-apart basins associated with double-overstepped left-lateral wrenches, although up to now, no major strike-slip fault which might have caused rifting in the Gunsan Basin has been found. More recently, Ren et al. (2002) suggested similarities between intracontinental rift basins and the South Yellow Sea Basin.

The purpose of this paper is to establish some details of the tectonic evolution of the Gunsan Basin. For the analysis, this study focuses on backstripping the subsidence history of the basin, which is useful for investigating the basin-forming mechanisms. One of the benefits of a complete decompaction and backstripping procedure is that the subsidence history of basins can be compared without the complications of different paleobathymetric, eustatic, compactional and isostatic effects (Allen and Allen, 2002).

## 2. Geologic Setting

East Asia comprises a mosaic of distinct continental fragments separated by fold belts resulting from the accretion of various fragments formerly separated by intervening areas of oceanic crust (Watson et al., 1987). The Yellow Sea lies on the Yangtze (South China) Platform and the Sino-Korean (North China) Platform, sutured by the Qinling-Dabie-Sulu collisional
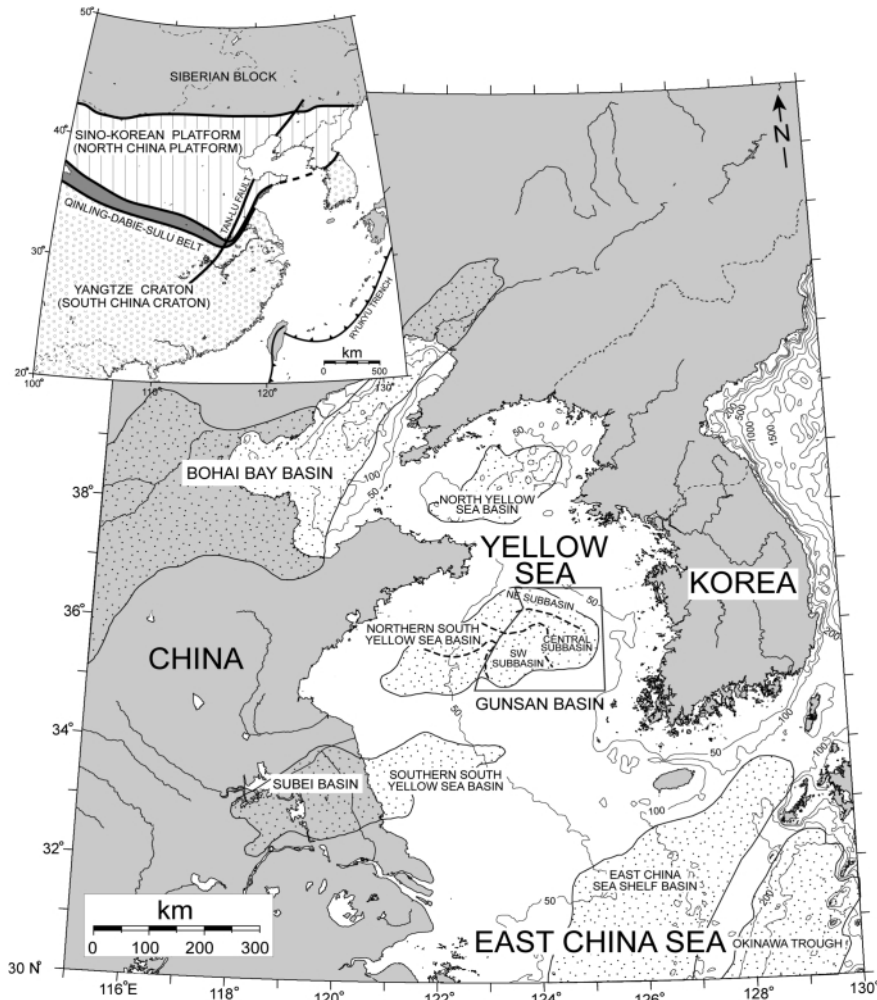
**FIGURE 1:** Bathymetry of the Yellow Sea, and major Cenozoic basins (modified from Lee et al., 2006). The Gunsan Basin is the Korean portion of the Northern South Yellow Sea Basin.



**FIGURE 2:** . Geological setting of the South Yellow Sea Basin, separated into Northern and Southern South Yellow Sea Basins by the Central High. The Gunsan Basin is the Korean portion of the Northern South Yellow Sea Basin in Korean shelf block 1 and 2. Locations of 5 exploratory wells (■) and 4 artificial well sites (●) for subsidence analysis (modified from PEDECO, 1997).

belt during the early Mesozoic (Hsu, 1989; Gilder and Courtillot, 1997; Kim et al., 2000; Wu, 2002).

Since late Mesozoic times, a large number extensional or transtensional basins have developed in East China, caused by large-scale interactions between the Pacific, Eurasian and Indian plates (Ren et al., 2002). In the Gunsan Basin, which formed on the Yangtze Platform (Fig. 1), rifting started in the late Mesozoic times. At 65 Ma, during the early Late Cretaceous, the Pacific Plate moved to the edge of eastern China and changed its subduction velocity and direction from NNW to WNW, at a steep angle (Uyeda and Kanamori, 1979; Engebretson et al., 1985; Maruyama et al., 1997). These changes led to an upwelling of the asthenosphere and consequent thinning of the lithosphere in eastern China (Yu et al., 2008, Zhou and Li, 2000), assisting the rifting process in eastern Eurasia and resulted in Late Cretaceous extensional tectonics.

The Gunsan Basin is divided into three sub-basins by basement highs and faults; the North-East (NE), Central and South-West (SW) sub-basins (Yi et al., 2003; KIGAM, 2006) (Fig. 2). The structure of the North-East sub-basin is difficult to characterize its structure due to problems with defining its exact northeastern border: here, a few NW-SE trending normal faults have been recognized on seismic profiles close to the presumed basin margin. The NW-SE trending Central sub-basin, which lies between basement highs separating it from the NE and SW sub-basins, is further characterized by a different structural style than in the regions to the north and south. In the south, it is a sag type basin with gently sloping boundaries, whereas in the north it is defined as a half-graben structure with a rotated hanging wall relatively down-thrown at the bounding normal faults. The South-West sub-basin includes both graben and half-graben structures that developed along the E-W trending
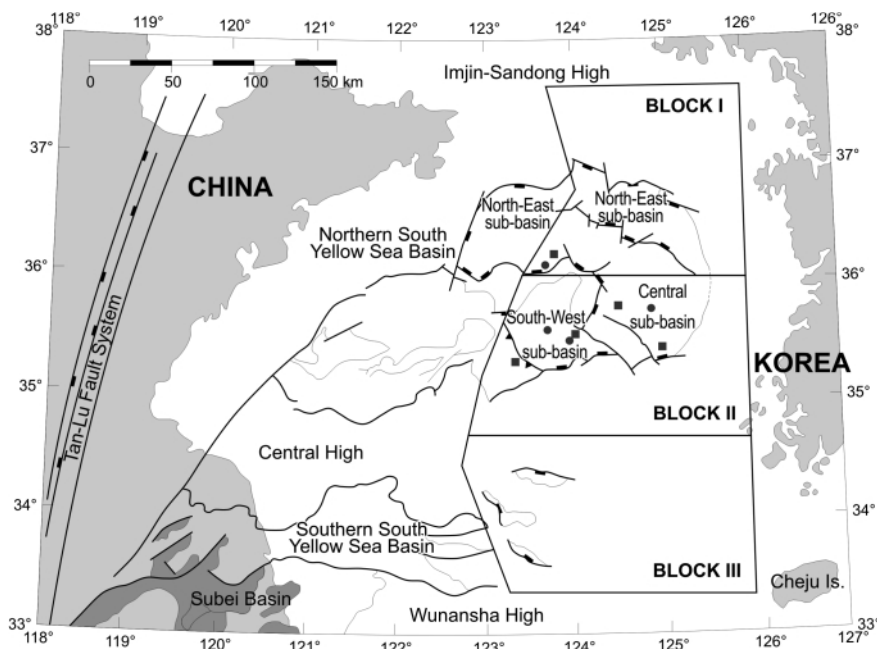
southern bounding faults (Shin et al., 2005).

The sediment fill of the Gunsan Basin mainly consists of Upper Cretaceous and Cenozoic non-marine (fluvial-alluvial and lacustrine) clastic sediments with a thickness of several kilometers. Erosion of the sediments deposited within the basin occurred during the Oligocene to Early Miocene, when the basin was subjected to compression and inversion. Since the middle Miocene, deposition has been dominated by mainly unconsolidated sands (KIGAM, 2006, Yi et al., 2003).

## 3. Data and Methods

Backstripping is a technique for progressively removing the sedimentary load from a basin, correcting for compaction, paleobathymetry and changes in sea level, in order to reveal the tectonic driving mechanisms of basin subsidence. The procedure for backstripping a sedimentary basin starts with the division of the stratigraphic column into increments for which the thickness and age range can be accurately determined (Miall, 2000).
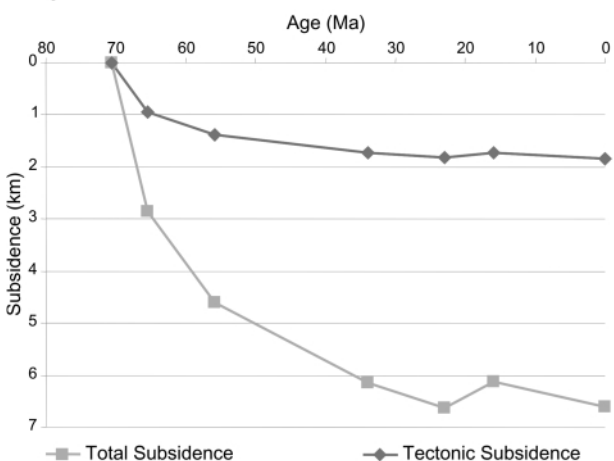
This technique requires an inference on the variation of porosity with depth, to enable the decompaction of stratigraphic units to be calculated. This is taken to be a simple exponential decrease with increasing depth, z, $\emptyset = \emptyset_o \exp(-cz)$ ($\emptyset_o$: the initial porosity, c: the porosity-depth coefficient) (Sclater & Christie, 1980). Further, following Steckler & Watts (1978), water-loaded basement subsidence, Y, is given by $Y = S[(\rho_m-\rho_s)/(\rho_m-\rho_w)] + W_d - \Delta_{SL}[\rho_m/(\rho_m-\rho_w)]$ (S: sediment layer thickness corrected for compaction, $\Delta_{SL}$: sea-level change, Wd: water depth, at burial time. $\rho_m$, $\rho_s$, and $\rho_w$: the mantle, mean sediment, and water densities).
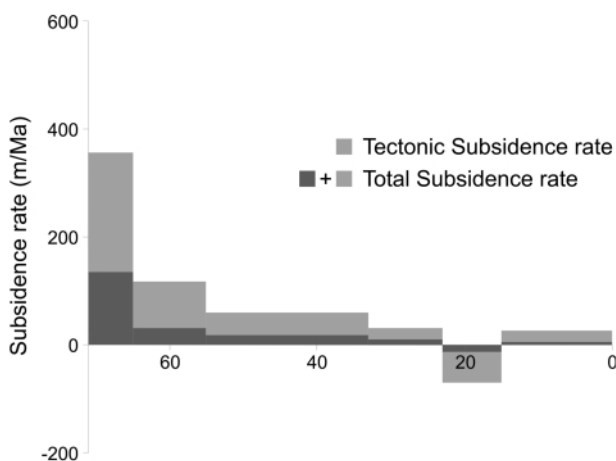
The data for this work were collected by the Korea National Oil Company (KNOC) and Korea Institute of Geoscience and Mineral (KIGAM). The geological ages of the key unconformity surfaces (acoustic basement, top of the Upper Cretaceous (Maastrichtian), top of the Paleocene, top of the Eocene, bottom of the Middle Miocene) recognized on seismic data were taken directly from KIGAM (2006) and Park et al. (2005), which are based on data from exploration wells (IIC-1X, IIH-1Xa, Haema, Inga, and Kachi) in the Gunsan Basin.

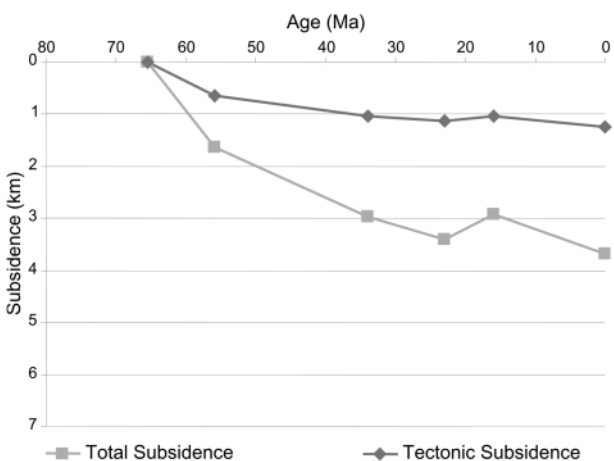In this area, porosity values calculated from the available
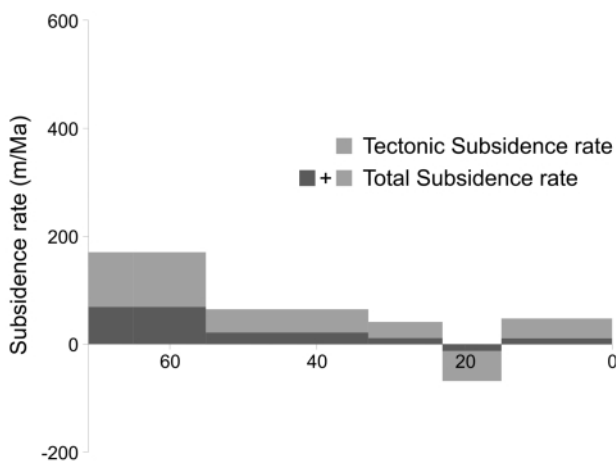


**Figure 3:** Subsidence history and rates of sag and half-graben structures in the Central sub-basin.

| Lithology | $\varnothing_o$ | c (x $10^{-3}$cm$^{-1}$) | $\rho_{sg}$ (g/cm$^{-3}$) |
|---|---|---|---|
| Shale | 0,63 | 0,51 | 2,72 |
| Sand | 0,49 | 0,27 | 2,65 |
| Chalk | 0,70 | 0,71 | 2,71 |
| Shaley Sand | 0,56 | 0,39 | 2,68 |

**Table 1:** Exponents of Surface porosity ($\varnothing_o$), Porosity-depth coefficient (c), Sediment grain density ($\rho_{sg}$) for different lithologies (modified from Sclater & Christie, 1980).

well data are not applicable because the results are unrealistically high. Thus typical values for the subsurface porosity and the porosity-depth coefficient were taken from published general exponent data (Tab. 1). In this study, $\Delta_{SL}$ and $W_d$ parameters used for water-loaded basement subsidence, were not considered, because the Gunsan Basin sediments are nonmarine with shallow paleobathymetries and negligible influences from sea-level changes. For this backstripping, the above processes were calculated on a spreadsheets using of Microsoft Excel.

To reconstruct the thickness of sediment eroded during the Early Miocene, the stratum thickness trend on eroded tilted fault blocks on the seismic section of the Central sub-basin were analyzed, based on the typical tectonic and stratigraphic evolution. From this, the eroded thickness was estimated at about 500 m.

## 4. Subsidence analysis of the Gunsan Basin

To analyze the subsidence history, four "artificial wells" were selected from typical seismic profiles of representative units in the Gunsan Basin: these are the southern sag and northern half-graben structures in the Central sub-basin, and half-graben and graben structures in the SW sub-basin (Fig. 2).
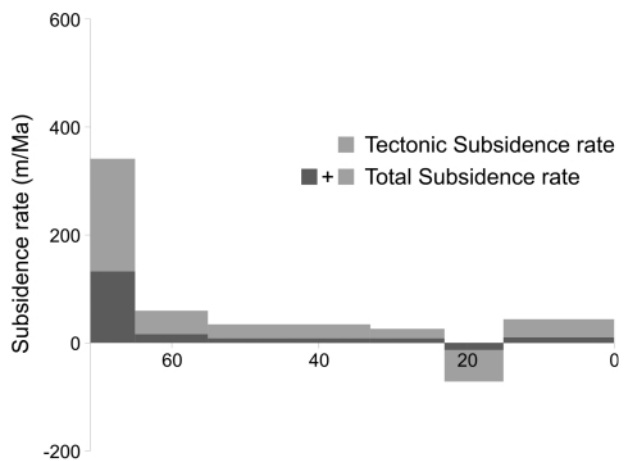
### 4.1 Subsidence analysis in the Central sub-basin

In the Central sub-basin, the southern sag and northern half-graben structures are selected for reconstruction of the subsidence history. The subsidence curves of the southern sag structure can be divided into 6 segments (Fig.3): 1) Late Cre-

• Half-graben structure in the SW sub-basin
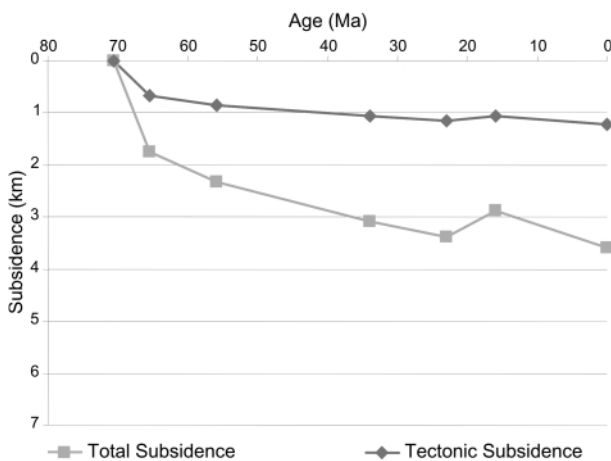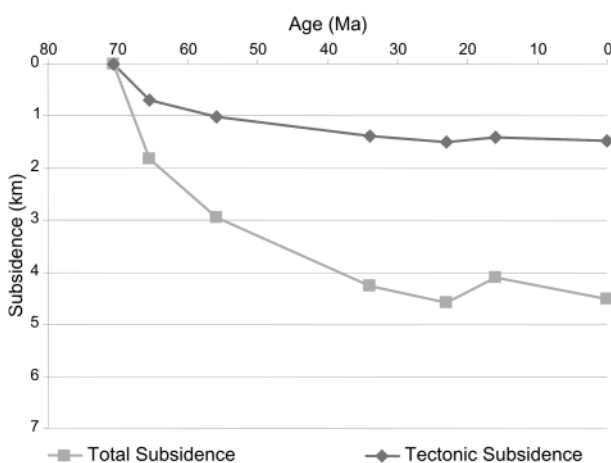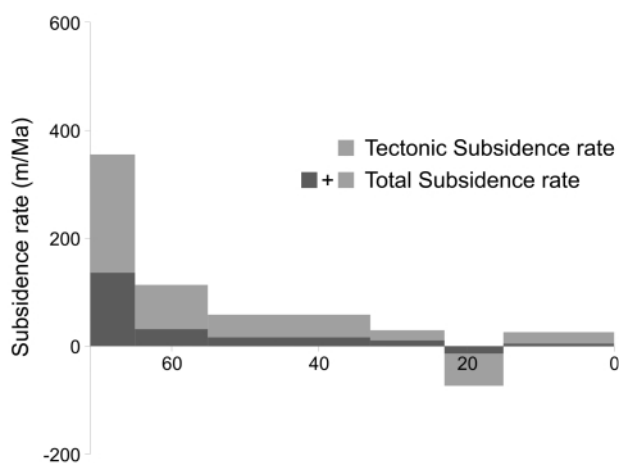


(a) Subsidence history

(b) Subsidence rate

• Graben structure in the SW sub-basin



(a) Subsidence history

(b) Subsidence rate

**Figure 4:** Subsidence history and rates of half-graben and graben structures in the SW sub-basin.

taceous (Maastrichtian) (70.6-65.5 Ma), 2) Paleocene (65.5-55.8 Ma), 3) Eocene (55.8-33.9 Ma), 4) Oligocene (33.9-23.03 Ma), 5) Early Miocene (23.03-15.97 Ma), 6) Middle Miocene-Present (15.97-0 Ma). During the Late Cretaceous, the subsidence curves are very steep, with subsidence rates of ca. 558 m/Ma for total subsidence and ca. 187 m/Ma for tectonic subsidence. Paleocene subsidence curves are also steep, with subsidence rates of ca. 182 m/Ma for total subsidence and ca. 45 m/Ma for tectonic subsidence. On the whole, sub-sidence rates decrease gradually to ca. 45 m/Ma for total sub-sidence and ca. 9 m/Ma for tectonic subsidence from the Late Creta-ceous to Oligocene. In the Early Miocene, the curves rise and show uplift and erosion. Again, from the Middle Miocene on-wards, this structure subsides at a rate of ca. 30 m/Ma for to-tal subsidence and ca. 7 m/Ma for tectonic subsidence.

The subsidence curves of the northern half-graben structure can be divided into 5 segments (Fig. 3). Compared with the subsidence curves in the southern structure of this sub-basin, the subsidence curves in the north have no Late Cretaceous segment. Subsidence started in the Paleocene with steep su-bsidence curves indicating a subsidence rate of ca. 169 m/Ma for total subsidence and ca. 67 m/Ma for tectonic subsidence. Similar to the southern part, in the Oligocene, the subsidence rate decreased steadily to ca. 41 m/Ma for total subsidence and ca. 8 m/Ma for tectonic subsidence. In the Early Miocene, uplift and erosion occurred, but from the Middle Miocene on-wards, subsidence started again.

## 4.2 Subsidence analysis in the SW sub-basin

In the SW sub-basin, half-graben and graben structures are selected for calculation of the subsidence history. The subsi-dence curves of these two structures can be divided into 6 segments (Fig. 4): 1) Late Cretaceous (Maastrichtian) (70.6-65.5 Ma), 2) Paleocene (65.5-55.8 Ma), 3) Eocene (55.8-33.9 Ma), 4) Oligocene (33.9-23.03 Ma), 5) Early Miocene (23.03-15.97 Ma), 6) Middle Miocene-Present (15.97-0 Ma).

In both the graben and half-graben structures, the subsidence history shows a similar pattern. During the Late Cretaceous, the subsidence curves are very steep, but become successi-vely gentler towards the Oligocene. This indicates gradually decreasing subsidence rates from Late Cretaceous to Oligo-cene times. During the Late Cretaceous, subsidence rates in the half-graben structure are ca. 341 m/Ma for total subsidence and ca. 132 m/Ma for tectonic subsidence. This decreased to ca. 27 m/Ma and ca. 8 m/Ma, respectively, in the Oligocene. From the Late Cretaceous to the Oligocene, subsidence rates in the graben structure of ca. 357 m/Ma for total subsidence and ca. 136 m/Ma for tectonic subsidence decreased to ca. 30 m/Ma and ca. 10 m/Ma, respectively. During the Early Mio-cene, a rise in the curves indicates uplift and erosion, but from the Middle Miocene onwards, these structures started to subside again.

## 5. The subsidence history of the Gunsan Basin

The subsidence history of the Gunsan Basin is separated in-to a main subsidence phase during the Late Cretaceous-Oli-gocene and a secondary subsidence phase during the Middle Miocene-Present, by the uplift and erosional phase of the Ear-ly Miocene. The main subsidence phase consists of a rapid subsidence and a slow subsidence event (Fig. 7).
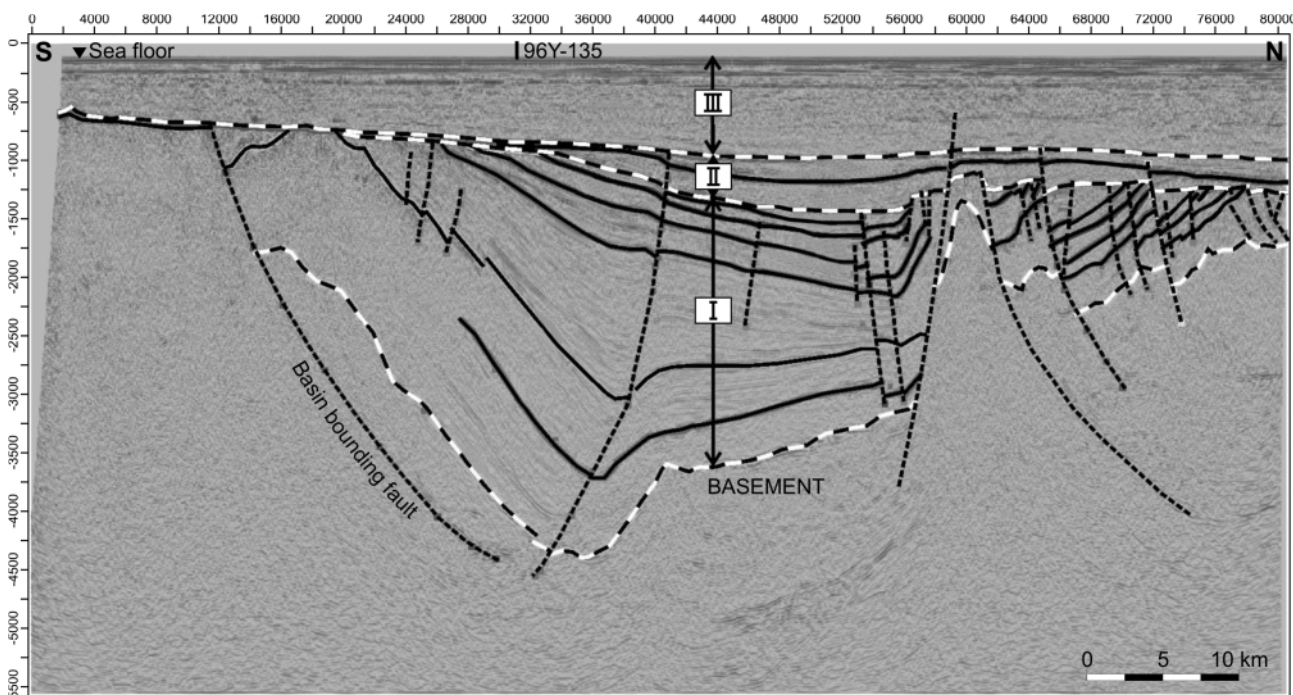


**Figure 5:** S-N direction seismic profile showing MSQ I (Acoutstic basement-Paleocene), II (Eocene), III (Middle Miocene-Present) in SW sub-basin (modified from Park et al., 2005).
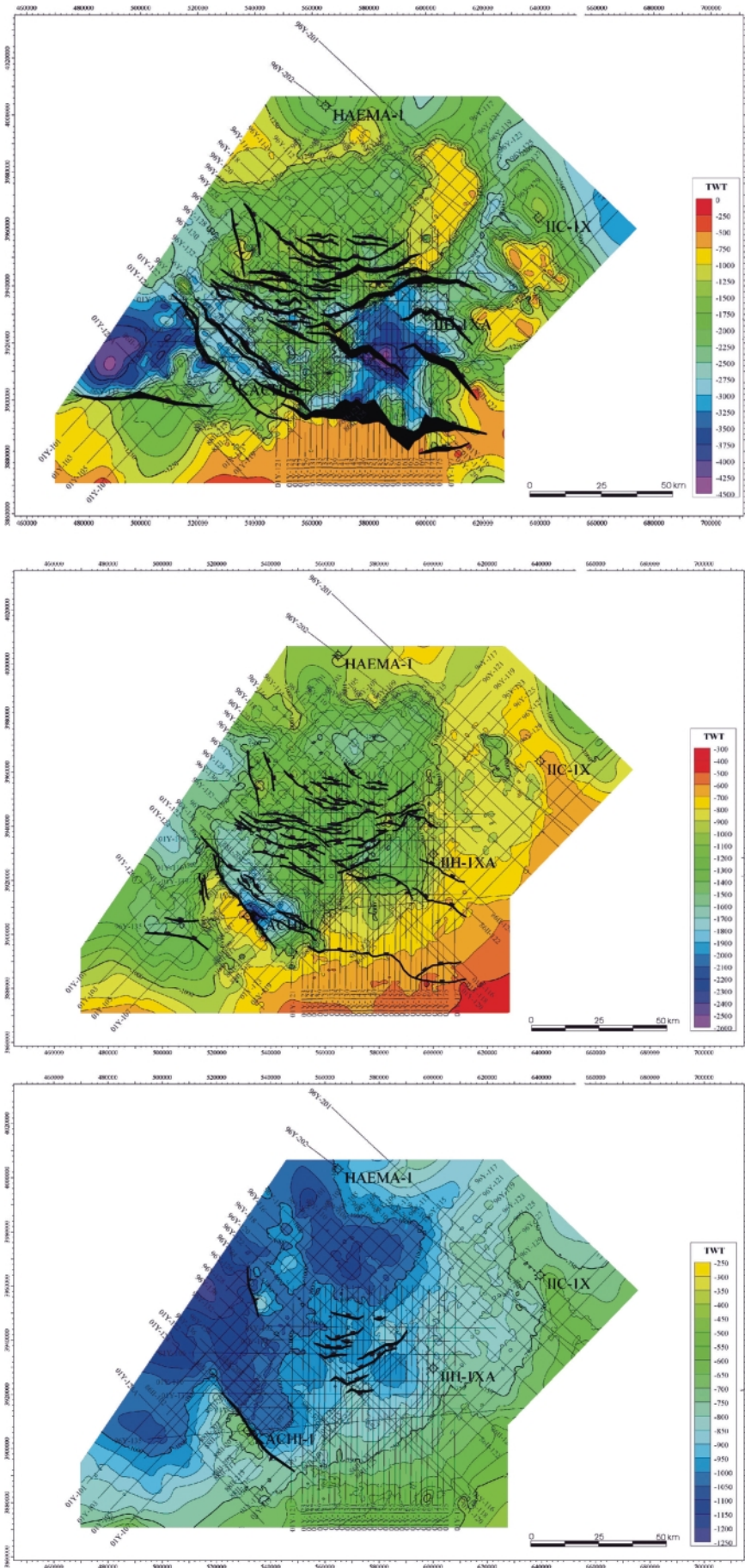
**FIGURE 6:** Time horizons structure maps of (a) top of basement, (b) late Paleocene unconformity, (c) late Eocene unconformity (base middle Miocene unconformity) (modified from Park et al., 2005).

From the Late Cretaceous to the Oligocene, the subsidence curves of the basin become less steep documenting a steady decrease in the subsidence rates. The subsidence up to Oligocene times includes > 90 % of the total and tectonic subsidence that occurred in the Gunsan Basin. Hence this period is defined as the main subsidence phase. Within this, a rapid subsidence event (Late Cretaceous-Paleocene) and a slow subsidence event (Eocene-Oligocene) occurred. Tectonic subsidence rates between 132-187 m/Ma occurred during the Late Cretaceous, and between 17-67 m/Ma during the Paleocene. Subsidence rates between ca. 8-18 m/Ma occurred in the Eocene-Oligocene.

The basin was inverted after the Oligocene, with erosion during the Early Miocene. This event defined as the uplift and erosion phase, terminated the main subsidence phase. Since the Middle Miocene, the basin has subsided again, at between ca. 5-12 m/Ma, defined as the secondary subsidence phase.

## 6. DISCUSSION

Park et al., (2005) and Shin et al., (2005) delineated the geologic structure and seismic stratigraphy in the SW sub-basin of the Gunsan Basin through an interpretation of 2D seismic data. These studies identified 12 unconformities in the SW subbasin and combined the formations into 3 mega-sequences; MSQ I (Late Cretaceous-Paleocene), MSQ II (Eocene) and MSQ III (Middle Miocene-Present) (Fig. 5). This classification corresponds to the subsidence phases identified in this study.

The Late Cretaceous-Paleocene rapid subsidence event is correlated with MSQ I which was interpreted as being formed from syn-rift sediments related to the development of faults during a N-S trending extensional stress regime (Shin et al., 2005). Most faults cut the Paleocene, but not the unconformably overlying Eocene (Fig. 6). This indicates

that the tectonic driving force of basin rifting was very strong in this period, and led to the high tectonic subsidence rates of the rapid subsidence event.

The Eocene-Oligocene slow subsidence event correlates with MSQ II (Eocene), which was characterized by post-rift sedimentation. In this event, most faults cut the basement and Paleocene, but are covered by the unconformably over-lying Eocene (Park et al., 2005, Shin et al., 2005) (Fig. 6). This indicates an abrupt decrease of tectonic driving force at the end of the Eocene, and is related to the low tectonic sub-sidence rates during the slow subsidence event.

Middle Miocene sediments unconformably overlie Eocene sediments in the SW sub-basin and Oligocene sediments in the Central sub-basin. Therefore, MSQ II does not include the Oligocene period. In this study, it was assumed that the Oli-gocene sediments originally deposited in the SW sub-basin were entirely eroded during the early Miocene. Therefore, in the subsidence analysis of the SW sub-basin, only Eocene and Miocene sediments were included. Another explanation for the lack of Oligocene sediments could be an earlier defor-

mation and uplift followed by erosion.

The secondary subsidence phase is equivalent to MSQ III (Middle Miocene-Present). After the middle Miocene, regional subsidence again led to widespread sedimentation. However, few faults developed and the seismic reflections within strata are consistent, parallel and continuous. This indicates that this period was marked by tectonic quiescence and uniform sedimentation.

Extension began in the latest Cretaceous along the east Eu-rasian plate boundary (Northrup et al. 1995). This correlates well with periods of reduced convergence rates between the Pacific plate and Eurasia. This suggests a slowing of the con-vergence rate between the Pacific and Eurasia plates during early and middle Cenozoic times, which may have been rela-ted to a decrease in the horizontal compressive stress trans-mitted between the Pacific and Eurasian plates, as reflected by widespread extension adjacent to the Eurasian margin at this time. Ren et al., (2002) state that the Late Mesozoic and Cenozoic rift systems in eastern Asia lie between two of the most dynamic tectonic domains of the Earth's lithosphere: the subduction zones of the western Pa-cific and the Tethys-Himalayan oro-gen. The direction and rate of sub-duction from the Pacific side and subduction/collision along the Tethys domain have changed several times since the Mesozoic, which caused the variation of stress fields in eas-tern Eurasia in space and time. Rif-ting in eastern Eurasia was caused by changes of convergence rate and direction in Pacific-Eurasia and India-Eurasia movements.

Fig. 7 compares the subsidence history of the Gunsan Basin with the convergence rates of the major tec-tonic plate boundaries. The Late Cre-taceous convergence rate of the Pa-cific-Eurasia plates was 120-140 mm/year (Engebretson et al., 1985; North-rup et al., 1995), when the stress field of eastern Asia was characterized by sinistral transpression (Tian and Du, 1987). The convergence rate decli-ned substantially during the early Cenozoic and reached a minimum of 30-40 mm/year in the Eocene. In contrast, the Late Cretaceous con-vergence rate of the India-Eurasia plates was about 100-110 mm/year and increased during the early Ce-nozoic and reached a maximum in the Paleocene of 170-180 mm/year at 65 Ma (Lee and Lawver, 1995). This period corresponds to the ear-
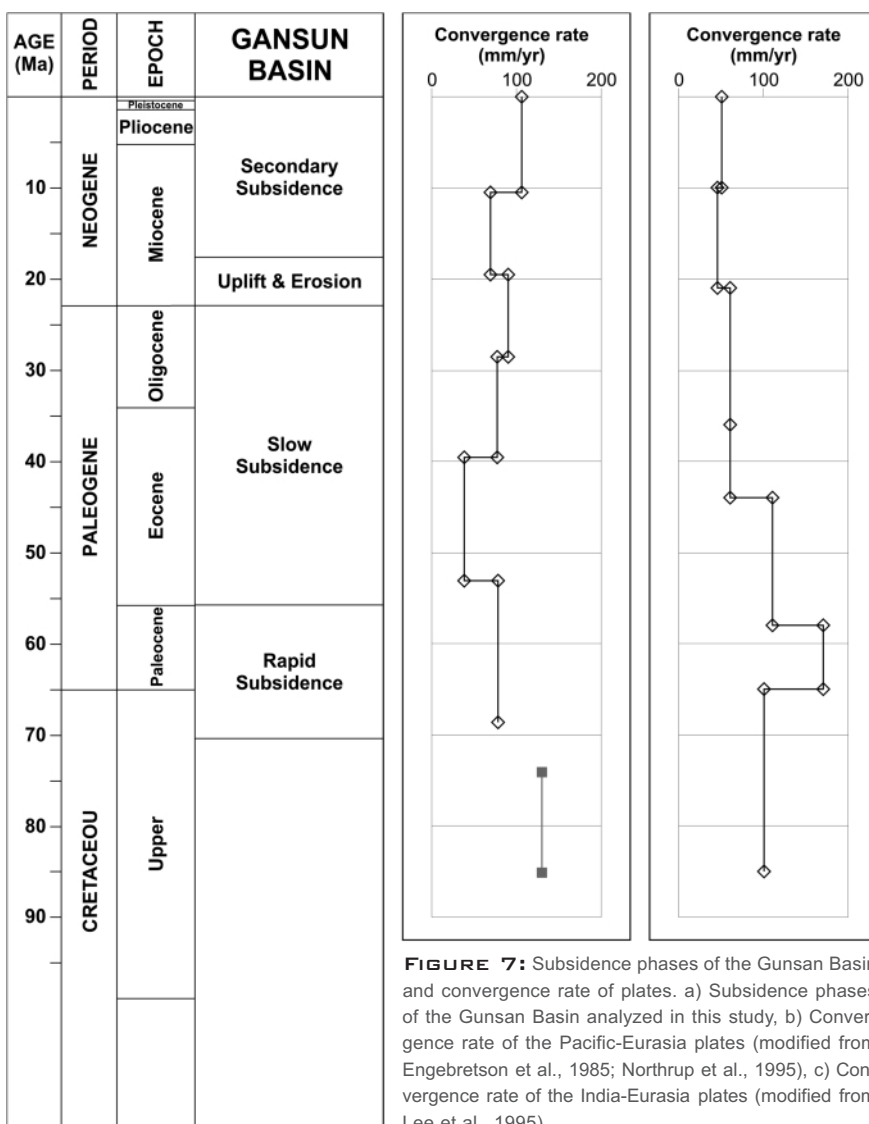


**FIGURE 7:** Subsidence phases of the Gunsan Basin and convergence rate of plates. a) Subsidence phases of the Gunsan Basin analyzed in this study, b) Conver-gence rate of the Pacific-Eurasia plates (modified from Engebretson et al., 1985; Northrup et al., 1995), c) Con-vergence rate of the India-Eurasia plates (modified from Lee et al., 1995).
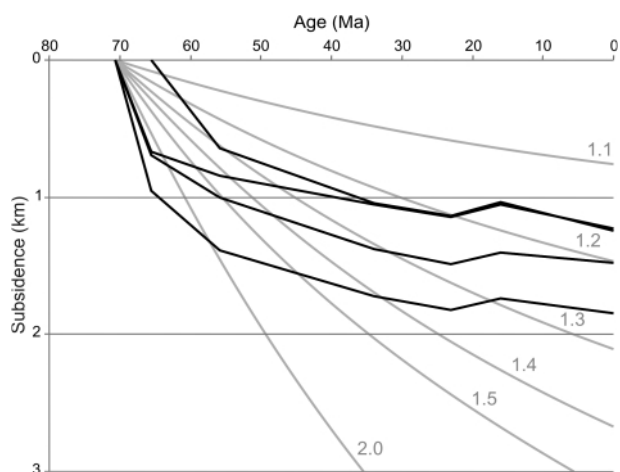
**FIGURE 8:** Comparison of tectonic subsidence curves of the Gunsan Basin (from Fig. 3 and 4) with post-rift thermal subsidence curves calculated from McKenzie (1978). Black lines are the tectonic subsidence curves of the Gunsan Basin and gray lines are for thermal subsidence curves calculated for differing β values.

ly Cenozoic rapid syn-rifting period of Eastern China (Ren et al., 2002). In the Gunsan Basin, it corresponds to the rapid subsidence and slow subsidence events, the former event, in particular, is equivalent to an abrupt decrease of convergence rate between the Pacific and Eurasia plates during the Late Cretaceous and increase of convergence rate between the India and Eurasia plates during the Paleocene (Fig. 7).

From Late Oligocene to Neogene times, the Pacific–Eurasia convergence rate increased to an average of 100-110 mm/year (Northrup et al., 1995), and the India-Eurasia convergence rate decreased to 50 mm/year (Lee and Lawver, 1995). In this period, extension stopped in eastern Asia, and many rift systems in East China gradually evolved into a thermal subsidence stage (Ren et al., 2002). And here, starting in the Late Eocene time, NNW movement of the Pacific plate changed to WNW movement, due to the termination of oceanic subduction beneath the India-Eurasia collision zone (Ren et al., 2002, Patriat and Archache, 1984). This corresponds to the uplift and erosion phase and the secondary subsidence phase of the Gunsan Basin (Fig. 7).

The tectonic subsidence curves of the Gunsan Basin (Fig. 3 and 4) are compared with the McKenzie (1978) lithospheric stretching model in Fig. 8. The modeled curves were calculated for post-rift thermal subsidence resulting from lithospheric re-equilibration after stretching and thinning. Tectonic subsidence in the Gunsan Basin was less than 2 km, with subsidence curves approximately exponential in shape, and progressing to simple thermal subsidence models of stretching factors ranging from 1.1 to 1.3. Following Xie and Heller (2009), strike-slip basins are characterized by rapid and short-lived (typically <10 m.y.) subsidence, but intracontinental basins have relatively slow and long-lived (typically >200 m.y.) subsidence histories. Further, most tectonic subsidence curves compiled from intracontinental basins show < 2 km subsidence, approximately exponential in shape and broadly consistent with simple thermal subsidence models of stretching factors (β)

ranging from 1.1 to 1.5 (Xie and Heller, 2009).

# 7. CONCLUSIONS

1) The Gunsan Basin, located between East China and West Korea, is filled with mainly Upper Cretaceous and Cenozoic non-marine clastic sediments. To analyze the subsidence history, four sites were selected from representative tectonic units, which comprise sag and half-graben structures in the Central sub-basin and half-graben and graben structures in the SW sub-basin.

2) The subsidence history of the Gunsan Basin is grouped into 3 phases; a main subsidence phase (Late Cretaceous-Oligocene), an uplift and erosion phase (Early Miocene), and a secondary subsidence phase (Middle Miocene-Present). Further, the main subsidence phase consists of a rapid subsidence (Late Cretaceous-Paleocene) and a slow subsidence event (Eocene-Oligocene).

3) Compared with seismic stratigraphy studies of the SW sub-basin, the rapid subsidence phase is equivalent to seismic sequence MSQ I (Late Cretaceous-Paleocene) and is interpreted as a period of syn-rift sedimentation. The slow subsidence phase corresponds to MSQ II (Eocene) which was characterized by post-rift sedimentation. The secondary subsidence phase is equivalent to MSQ III (Middle Miocene-Present).

4) The evolution of the Late Mesozoic and Cenozoic rift systems in eastern Asia may be linked to the convergence rates of the Pacific-Eurasia and also the India-Eurasia plates. The subsidence history of the Gunsan Basin shows that the main subsidence phase occurred during a decreasing convergence rate of the Pacific-Eurasia plates and an increasing convergence rate of the India-Eurasia plates. The uplift and erosion phase and the secondary subsidence phase are related to increasing convergence rate of the Pacific-Eurasia plates and a decreasing convergence rate of the India-Eurasia plates.

5) Tectonic subsidence curves of the Gunsan Basin show less than 2 km subsidence, approximately exponential in shape and progressing to simple thermal subsidence models of stretching factors ranging from 1.1 to 1.3. This is relatively similar to the typical tectonic subsidence characteristics of intracontinental basins, rather than strike-slip basins.

## References

Allen, P.A. and Allen, J.R., 2005. Basin Analysis: Principles and Applications. Blackwell Scientific Publications, pp. 549.

Baag C. and Baag, C.-E., 1998. Aeromagnetic interpretation of southwestern continental shelf of Korea. In: Gibson, R.I., Millegan, P.S. (Eds.), Geologic Applications of Gravity and Magnetics: Case Histories. Society of Exploration Geophysicists Geophysical References Series 8, pp. 63–68.

Engebretson, D.C., Cox, A. and Gordon, R.G., 1985. Relative Motions Between Oceanic and Continental Plates in the Pacific Basin. The Geological Society of America, Special Paper, 206, 1–59.

Gilder, S. and Courtillot, V., 1997. Timing of the North-South China collision from the middle to late Mesozoic paleomagnetic data from the North China Block. Journal of Geophysical Research 102 (B8), 17713–17727.

Hsu, K.J., 1989. Origin of sedimentary basins of China. In: Zhu, X. (Ed.), Chinese Sedimentary Basins. Sedimentary Basins of the World 1. Elsevier, New York, pp. 208–227.

KIGAM, 2006. Joint Study on Sedimentary Basins between Korea and China. Korea Institute of Geoscience And Mineral Report GAA2003002-2006(4) (in Korean, with English abstract).

Kim, J.-N., Ree, J.-H., Kwon, S.-T., Park, Y., Choi, S.-J. and Cheong, C.-S., 2000. The Kyonggi shear zone of the central Korean Peninsula: late orogenic imprint of the North and South China collision. The Journal of Geology 108, 469–478.

Lee, G.H., Kown, Y.I., Yoon, C.S., Kim, H.J., and Yoo, H.S., 2006. Igneous complexes in the Southeastern Northern South Yellow Sea Basin and their hydrocarbon Implications. Marine and petroleum Geology, 23, 631-645.

Lee, T.Y. and Lawver, L.A., 1995. Cenozoic plate reconstruction of Southeast Asia. Tectonophysics 251, 85-138.

Marathon, 1987. The geology and petroleum potential of Block II, volume I-IV.

Maruyama, S., Isozaki, Y. and Kimura, G., et al., 1997. Paleogeographic maps of the Japanese Islands: plate tectonic synthesis from 750 Ma to the present. Island Arc 6, 121–142.

McKenzie, D.P., 1978. Some remarks on the development of sedimentary basins: Earth and Planetary Science Letters 40, 25–32.

Miall, A.D., 2000. Principles of sedimentary basin analysis: Springer-Verlag, Berlin, 616 p.

Northrup, C.J., Royden, L.H. and Burchfiel, B.C., 1995. Motion of the Pacific plate relative to Eurasia and its potential relation to Cenozoic extension along the eastern margin of Eurasia. Geology 23, no. 8, 719-722.

Park, K.S., Park, K.P., Sunwoo, D., Yoo, D.G., Cheong, T.G., Oh, J.H., Bong, P.Y., Son, J.D., Lee, H.Y., Ryu, B.J., Son, B.K., Hwang, I.G., Kwon, Y.I., Lee, Y.J. and Kim, H.J., 1997. Petroleum resources assessment of the western part of the Kunsan Basin. KR-97(C)-17. KIGAM Research Report, Korean Institute of Geology, Mining and Materials, pp. 5-190 (in Korean, with English abstract).

Park, K.S., Kang, D.H., Shinn, Y.J. and Shin, J.B., 2005. Tectonic evolution of the western Kunsan Basin, Yellow Sea, offshore Korea. Journal of the Geological Society of Korea 41, 141–155 (in Korean with English abstract).

Patriat, P., and Achache, J., 1984. India-Asia collision chronology has implications for crustal shortening and driving mechanisms of plates. Nature 311, 615-621.

PEDCO, 1997. '96 Report of Geophysical Interpretation on South-West Sub-basin, Yellow Sea, Korea. Korea Petroleum Development Corporation (in Korean).

Ren, J., Tamaki, K., Li, S., and Junxia, Z., 2002. Late Mesozoic and Cenozoic rifting and its dynamic setting in Eastern China and adjacent areas. Tectonophysics 344, 175-205.

Sclater, J. G., and Christie P. A. F., 1980. Continental stretching: An explanation of the post-mid-Cretaceous subsidence of the central North Sea Basin. Journal of Geophysics Research 85, 3711-3739.

Shin, J.-B., Park, K.-S., Shinn, Y.-J. and Kang, D.-H., 2005. Analysis of Geologic Structure for the Seismic Data in the Block II of Kunsan Basin, Offshore Korea. KIGAM Bulletin 9, No.1, pp.72-83.

Steckler, M. S., and Watts A. B., 1978. Subsidence of the Atlantic-type continental margin of New York. Earth and Planetary Science Letters 41, 1-13.

Tian, Z.-Y. and Du, Y., 1987. Formation and evolution of the Yilan-Yitong graben. Tectonophysics 133, 165-173.

Uyeda, S. and Kanamori, H., 1979. Backarc opening and the mode of subduction. Journal of Geophysical Research 84, 1049–1061.

Watson, M.P., Hayward, A.B., Parkinson, D.N. and Zhang, Zh. M., 1987. Plate tectonic history, basin development and petroleum source rock deposition onshore China. Marine and Petroleum Geology 4, 205-225.

Wu, S., 2002. Mesozoic-Cenozoic rifting and origins of the North Yellow Sea Basin. Continent–Ocean Interactions within the East Asian Marginal Seas. American Geophysical Union Chapman Meeting Abstracts, San Diego, CA, 10–14 November 2002, p. 42.

Xie, X. and Heller, P.L., 2009. Plate tectonics and basin subsidence history. Geological Society of America Bulletin 121, 55-64.

Yi, S., Yi, S., Batten, D.J., Yun, H. and Park, S.-J., 2003. Cretaceous and Cenozoic on-marine deposits of the Northern South Yellow Sea Basin, offshore western Korea: palynostratigraphy and palaeoenvironments. Palaeogeography, Palaeoclimatology, Palaeoecology 191, 15–44.

Yu, Z., Wu, S., Zou, D., Feng, D. and Zhao, H., 2008. Seismic profiles across the middle Tan-Lu fault zone in Laizhou Bay, Bohai Sea, eastern China. Journal of Asian Earth Sciences 33, 383-394.

Zhang, Y., Wei, Z., Xu, W., Tao, R. and Chen, R., 1989. The North Jiangsu-South Yellow Sea Basin. In: Zhu, X. (Ed.), Chinese Sedimentary Basins. Elsevier, Amsterdam, pp. 107-123.

Zhou, X.M. and Li, X.W., 2000. Origin of late Mesozoic igneous rocks in southeastern China: implications for lithosphere subduction and underplating of mafic magmas. Tectonophysics 326, 269–287.

Eun Young LEE

Department Petroleum Resources Technology, University of Science & Technology,  Gwahangno 113, Yuseong-gu, Daejeon, South Korea;
Current address: Department of Geodynamics & Sedimentology, University of Vienna, Althanstrasse 14, 1090 Vienna, Austria;
queenily2@gmail.com